Binary Concentration Shift Keying with Multiple Measurements of Molecule Concentration in Mobile Molecular Communication

Yutaka Okaie(✉) and Tadashi Nakano

Osaka University Institute for Datability Science, Suita, Japan
yokaie@fbs.osaka-u.ac.jp, tnakano@ids.osaka-u.ac.jp

Abstract. Binary concentration shift keying in molecular communication is a modulation technique that transforms binary information onto the concentration of molecules. Transmitter releases a pre-specified number of molecules into the environment according to the information it wishes to transmit to receiver. In this paper, we consider binary concentration shift keying in mobile molecular communication where a mobile receiver performs multiple measurements of molecule concentration to demodulate information that the transmitter transmits. Numerical experiments are conducted to evaluate the performance of mobile molecular communication with the binary concentration shift keying with multiple measurements of molecule concentration in terms of achievable information transmission rate.

Keywords: Mobile molecular communication · Binary concentration shift keying · Multiple measurements

1 Introduction

In molecular communication, bio-nanomachines communicate by propagating diffusive molecules in the environment [4,5,11,12]. Bio-nanomachines in molecular communication are at the nano-to-micro meter in size, composed of biological materials, and capable of biochemical functionalities such as sensing a specific type of molecule. Bio-nanomachines in molecular communication are often mobile since their spatial positions fluctuate due to thermal noise [10]. Examples of bio-nanomachines are biological cells including genetically engineered cells. Molecular communication is more energy efficient and compatible with biological environments than existing telecommunication, and its application to medicine is anticipated [13].

In this paper, we consider binary concentration shift keying (BCSK) in molecular communication. In transmitting binary information, a transmitter bio-nanomachine releases the corresponding number of molecules into the environment. The released molecules propagate in the environment. A receiver

Y. Chen et al. (Eds.): BICT 2020, LNICST 329, pp. 42–51, 2020.
https://doi.org/10.1007/978-3-030-57115-3_4

bio-nanomachine performs multiple measurements of molecule concentration to demodulate information that the transmitter bio-nanomachine transmits. We also consider mobile molecular communication where the spatial position of the receiver bio-nanomachine fluctuates due to thermal noise [1,2,6,8].

The paper is organized as follows. In Sect. 2, we develop a mathematical model of the molecular communication described above. In this section, we also describe a mathematical model of molecular communication where a receiver bio-nanomachine performs a single measurement of molecule concentration [9]. In Sect. 3, we conduct numerical experiments and examine the impact of key model parameters on the performance of molecular communication. We use the achievable rate as a performance measure and compare the binary concentration shift keying with multiple measurements of molecule concentration and that with single measurement. Finally, we discuss the future work and conclude the paper in Sect. 4.

2 Molecular Communication Model

Figure 1 shows an overview of the molecular communication model, consisting of a transmitter bio-nanomachine (Tx) and a receiver bio-nanomachine (Rx). Tx is a single point source of molecules. Rx is a passive receiver and modeled as a three-dimensional sphere of radius a. Also, Rx moves randomly due to thermal noise.

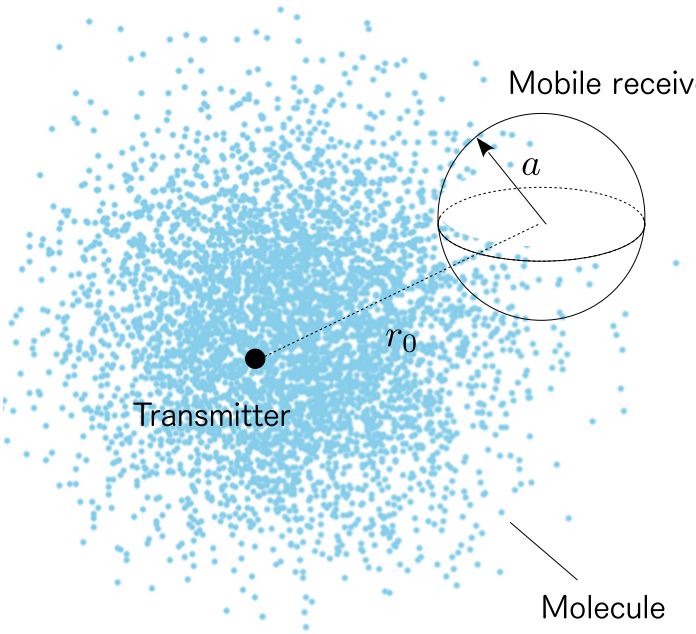

Fig. 1. Overview of the molecular communication model

In the model, we consider binary concentration shift keying (BCSK) for the modulation scheme, where the transmitted information symbol x is either "0" or "1". Tx sends information symbol x by releasing a pre-specified number of molecules, A_x, as a pulse wave into the three-dimensional environment. The concentration is A_1 for transmitting symbol "1", and A_0 for "0", respectively where $A_1 > A_0 > 0$ is assumed.

The center location of Rx is initially r_0 distance away from Tx, and the concentration of molecules at the center location of Rx after time t is

$$h_x(r_0; t, D_e) = \frac{A_x}{(4\pi D_e t)^{3/2}} \exp\left[-\frac{r_0^2}{4D_e t}\right], \tag{1}$$

where D_e is the effective diffusion coefficient given by the diffusion coefficient D_r of Rx and the diffusion coefficient D_m of signal molecules: $D_e = D_r + D_m$ [1]. Note that, by using the concept of effective diffusion coefficients, mobile molecular communication is transformed into static one where molecules diffuse with the effective diffusion coefficient and the location of Rx is fixed.

Rx is assumed to be a perfectly monitoring sphere, meaning that Rx is able to count the number of molecules within the volume of Rx without capturing the molecules. The number of molecules Rx receives at time t is given by

$$N_x(t; r_0) = V \times h_x(r_0; t, D_e), \tag{2}$$

where $x \in \{0, 1\}$ and V is the volume of Rx. We assume that r_0 is sufficiently large enough for molecules to distribute uniformly around Rx.

When molecules move randomly due to thermal noise, the number of molecules Rx receives fluctuates. We express the number $\hat{N}_x(t)$ of molecules that Rx receives in the presence of noise, using the normal distribution [7]:

$$\hat{N}_x(t) \sim \mathcal{N}\left(N_x(t), N_x(t)\right). \tag{3}$$

Through demodulation, Rx decides whether the symbol received Y is either "0" or "1" based on the number of molecules received, $\hat{N}_x(t)$, within a period of time T, i.e., $\left\{\hat{N}_x(t)\right\}_{0<t\leq T}$. A simple demodulation scheme is to detect the maximum concentration $\hat{N}_{\max} = \max_{0<t\leq T}\left\{\hat{N}_x(t)\right\}$, and compare it with a threshold number of molecules, ω; when $\hat{N}_{\max} > \omega$, $Y = 1$, and $Y = 0$ otherwise.

In this paper, we determine ω such that ω minimizes the sum of error probabilities as follows. When $\hat{N}_{\max}$ follows probability distribution $g_0(n)$ for $x = 0$, or $g_1(n)$ for $x = 1$, the error probability is expressed as

$$\begin{aligned} e(\omega) &= P_{Y|X}(1|0) + P_{Y|X}(0|1) \\ &= \int_{\omega}^{+\infty} g_0(\omega)\mathrm{d}\omega + \int_{-\infty}^{\omega} g_1(\omega)\mathrm{d}\omega. \end{aligned} \tag{4}$$

The necessary condition for ω to minimize $e(\omega)$ satisfies

$$\frac{\mathrm{d}}{\mathrm{d}\omega} e(\omega) = g_1(\omega) - g_0(\omega) = 0. \tag{5}$$

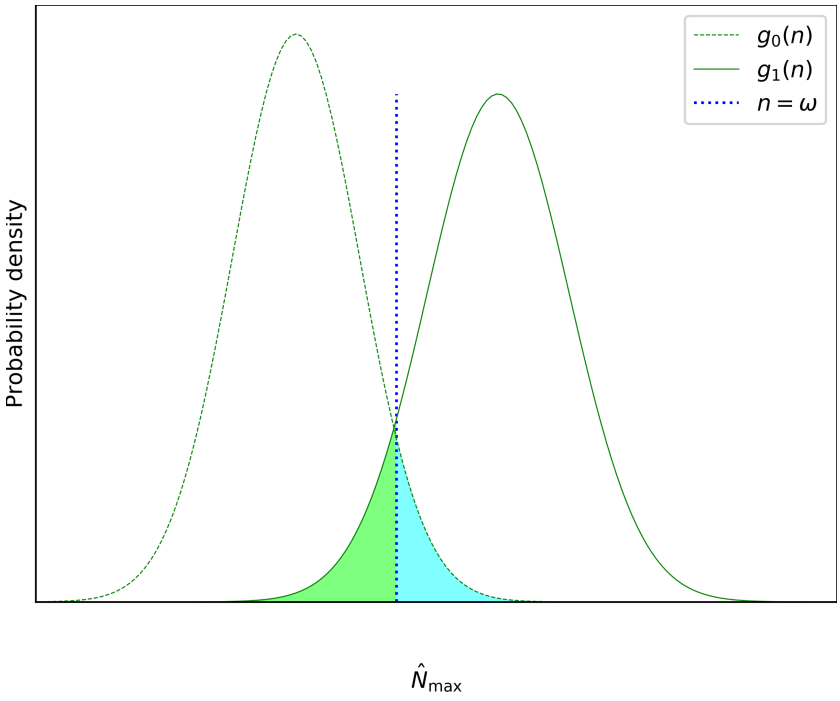

Fig. 2. Example plot of $g_0(n)$ and $g_1(n)$, and corresponding ω

Figure 2 shows example plots of $g_0(n)$ and $g_1(n)$, and corresponding ω. It shows that $e(\omega)$ coincides with an intersectional area between $g_0(n)$ and $g_1(n)$.

In the following, we consider two measurement schemes for estimating $\hat{N}_{\max}$: the single measurement scheme and the multiple measurement scheme. In the single measurement scheme, Rx measures the number of molecules once at the time when the number of molecules is the largest and obtains $\hat{N}_{\max}$. In the multiple measurement scheme, Rx measures the number of molecules multiple times at a constant time interval, and then obtains $\hat{N}_{\max}$ as the maximum number of molecules among the multiple measurements.

2.1 Single Measurement of Molecule Concentration

In the single measurement scheme, Rx measures the number of molecules at the peak time or when the number of molecules becomes the largest. The peak time is given by the solution of the first derivative of (1) with respect to time t:

$$t_{\text{peak}} = \max_{0<t^*} \left\{ \left. \frac{\mathrm{d}h_x(r_0; t, D_e)}{\mathrm{d}t} \right|_{t=t^*} = 0 \right\}$$
$$= \frac{\sqrt{9D_e^2 + 4kr_0^2 D_e} - 3D_e)}{4kD_e}. \tag{6}$$

From (3), $\hat{N}_{\max}$ is drawn from the following normal distribution:

$$f(n;x) = \mathcal{N}\left(N_x(t_{peak};r_0), N_x(t_{peak};r_0)\right) = \frac{1}{\sqrt{2\pi N_x(t_{peak};r_0)}} \exp\left(-\frac{(n-N_x(t_{peak};r_0))^2}{2N_x(t_{peak};r_0)}\right). \quad (7)$$

2.2 Multiple Measurements of Molecule Concentration

In the multiple measurement scheme, Rx measures the number of molecules multiple times at a constant time interval, τ. The k-th measurement follows the probability distribution:

$$f_{k\tau}(n;x) = \frac{1}{\sqrt{2\pi N_x(k\tau;r_0)}} \exp\left(-\frac{(n-N_x(k\tau;r_0))^2}{2N_x(k\tau;r_0)}\right). \quad (8)$$

The cumulative probability distribution of the maximum number of molecules, $\hat{N}_{\max}$, is

$$G(m;x) = \Pr\left[\hat{N}_{\max} < m\right] = \Pr\left[\max_{k\in\{0,1,\cdots,\lfloor T/\tau\rfloor\}} \hat{N}_x(k\tau;r_0) < m\right] = \prod_{k=0}^{\lfloor T/\tau\rfloor} \int_{-\infty}^{m} f_{k\tau}(n;x)\mathrm{d}n = \prod_{k=0}^{\lfloor T/\tau\rfloor} F_{k\tau}(m;x), \quad (9)$$

where

$$F_{k\tau}(m;x) = \frac{1}{2}\left\{1 + \mathrm{erf}\left(\frac{m-N_x(k\tau;r_0)}{\sqrt{2N_x(k\tau;r_0)}}\right)\right\}. \quad (10)$$

Therefore, $\hat{N}_{\max}$ follows the probability distribution:

$$g(m;x) = \frac{\mathrm{d}}{\mathrm{d}m}G(m;x) = \sum_{j=0}^{\lfloor T/\tau\rfloor} f_{j\tau}(m;x) \prod_{k\in\{0\cdots\lfloor T/\tau\rfloor\},k\neq j} F_{k\tau}(m;x). \quad (11)$$

3 Numerical Results

In this section, we examine the impact of key parameters, the number of molecules that Tx transmits, A_0, and the measurement time interval, τ. By default, we use the following parameters: $D_m = 3600$ (μm^2/h), $D_r = 300$ (μm^2/h), $A_1 = 1 \times 10^5$ (1/μm^3), $A_0 = 8.0 \times 10^4$ (1/μm^3), and $T = 10$ (h). We obtain these values from [9].

For the measurement time interval τ, we determine the default value based on [3]: Rx is a perfectly monitoring sphere of radius a, the turnover time t_{turnover} for measuring diffusive molecules whose diffusion coefficient D is

$$t_{\text{turnover}} = \frac{2a^2}{D}. \tag{12}$$

For the range of $3600 \leq D \leq 36000$ (μm^2/h) assumed in [9] and a typical cell size of $a = 5$ (μm), $0.0014 \leq t_{\text{turnover}} \leq 0.014$ (h), we choose $\tau = 0.01$ (h).

We evaluate the performance of molecular communication using the achievable rate defined by

$$I_{XY} = \max_{P_X(0)} \sum_{x \in \mathcal{B}} \sum_{y \in \mathcal{B}} P_{XY}(x, y) \log \frac{P_{XY}(x, y)}{P_X(x) \cdot P_Y(y)}, \tag{13}$$

where $\mathcal{B} = \{0, 1\}$. Figure 3 shows the pairs of probability distributions, $f(n; 0)$ and $f(n, 1)$ in (7), and $g(n, 0)$ and $g(n, 1)$ in (11) under the default configuration. ω_f and ω_g, are determined to meet (5): $f(\omega_f; 0) = f(\omega_f; 1)$ and $g(\omega_g; 0) = g(\omega_g; 1)$. The figure shows numerical results when the default configuration is used. It shows that $\hat{N}_{\max}$ from the multiple measurements follows the distribution with larger mean and smaller variance than that from the single measurement. This figure indicates that the multiple measurement scheme leads to a higher achievable rate than the single measurement scheme, when the default configuration is used.

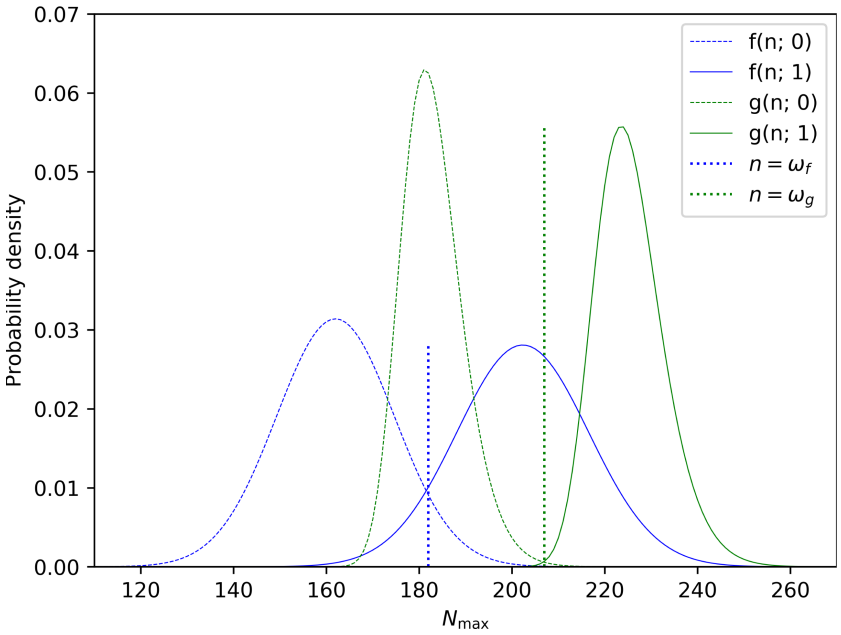

Fig. 3. $\hat{N}_{\max}$ distributions under default configuration

Figure 4 shows the impact of the effective diffusion coefficient D_e of molecules on the achievable rate with τ varied. We see that the achievable rate stays unchanged regardless of D_e in the single measurement scheme whereas it decreases in the multiple measurement scheme. In the single measurement scheme, as D_e increases, molecules diffuse more quickly reaching its peak in a shorter time at Rx, however, the number of molecules that Rx detects is constant, and thus results in the same achievable rate. In the multiple measurement scheme, as D_e increases, molecules dissipate in a shorter period of time, and the chance that Rx detects a large number of molecules decreases. Numerical results show that, as D_e increases, the achievable rate in the multiple measurement scheme decreases due to this effect. As the measurement time interval τ increases, the achievable rate in the multiple measurement scheme decreases since the chance of detecting a large number of molecules decreases. The same observation is made in the results to be presented below in this section (Fig. 5).

Figure 5 shows the impact of the number A_0 of molecules that Tx transmits on the achievable rate when $A_1 = 1.0 \times 10^5$ and τ is varied. As A_0 increases, the achievable rate decreases because the number of molecules that Rx measures for $x = 0$ and that for $x = 1$ become the same with a higher probability. Note that the ratio of A_0/A_1 represents the ability of Tx to differentiate the two symbols.

Figure 6 shows the impact of the measurement time interval τ. The single measurement scheme is not dependent on τ and the achievable rate in the single measurement scheme is constant with $t_{peak} = 0.43$ in this figure. In the

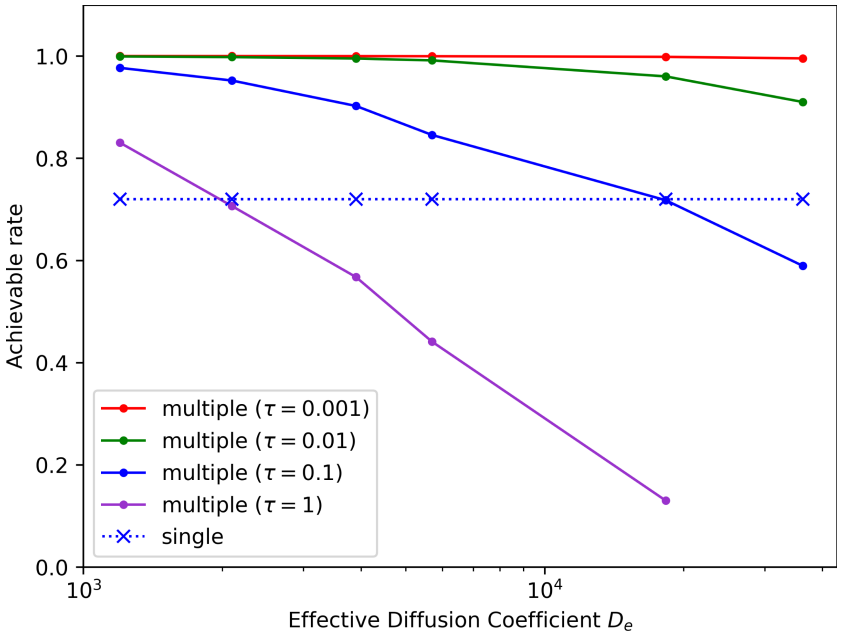

Fig. 4. Impact of the effective diffusion coefficient, D_e

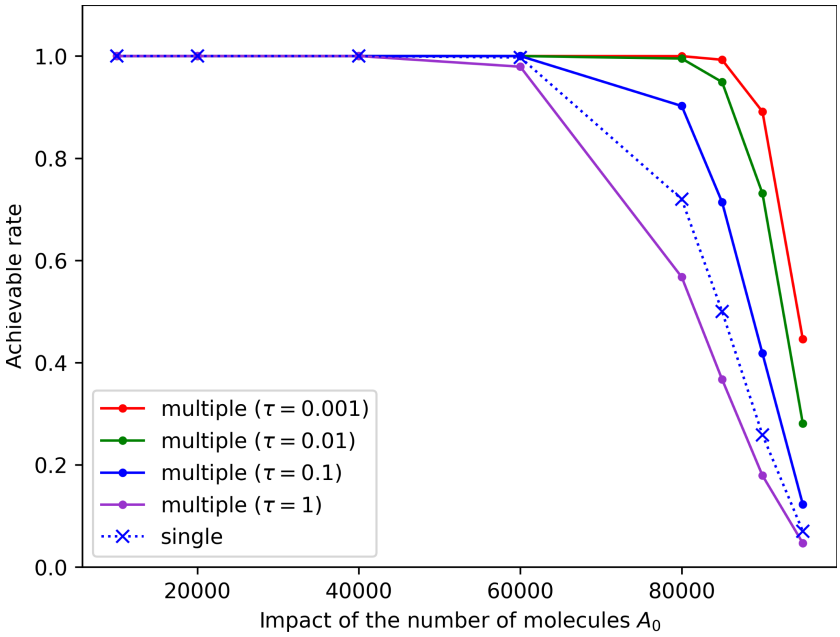

Fig. 5. Impact of the number of molecules that Tx transmits, A_0

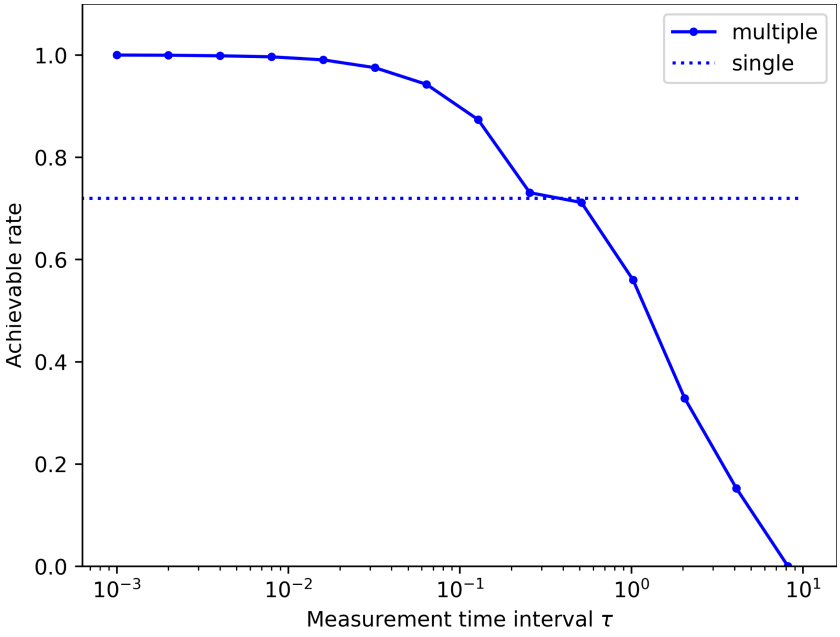

Fig. 6. Impact of the measurement time interval, τ

multiple measurement scheme, as τ increases, the achievable rate tends to decrease. This is because, as τ increases, the number of measurements that Rx performs decreases, and thus the chance that Rx detects a large number of molecules (e.g., the maximum number of molecules) decreases. The figure also shows that the single and multiple measurement schemes obtain the same achievable rate around $\tau = 0.4$.

4 Conclusion

In this paper, we computed the achievable rate of molecular communication where the binary concentration shift keying with multiple measurements of molecule concentration is employed. For comparison, we also computed the achievable rate of molecular communication where the binary concentration shift keying with single measurement of molecule concentration is employed.

In future work, we plan to consider transmission of multiple symbols in mobile molecular communication. In the molecular communication model in this paper, we focused on transmission of one symbol. We plan to extend the model to consider transmission of multiple symbols and consider the transmitter's motion and inter symbol interference (ISI) in mobile molecular communication [8]. In future work, we also consider other types of mobility such as directed motion and collective motion, and obtain the achievable rate of molecular communication.

Acknowledgment. This work was supported by JSPS KAKENHI Grant Number 18K18039 and 20K19784.

References

1. Ahmadzadeh, A., Jamali, V., Schober, R.: Stochastic channel modeling for diffusive mobile molecular communication systems. IEEE Trans. Commun. **66**(12), 6205–6220 (2018)
2. Cheng, Z., Zhang, Y., Xia, M.: Performance analysis of diffusive mobile multiuser molecular communication with drift. IEEE Trans. Mol. Biol. Multiscale Commun. **4**(4), 237–247 (2018)
3. Endres, R.G., Wingreen, N.S.: Accuracy of direct gradient sensing by single cells. Proc. Natl. Acad. Sci. **105**(41), 15749–15754 (2008)
4. Farsad, N., Yilmaz, H.B., Eckford, A., Chae, C., Guo, W.: A comprehensive survey of recent advancements in molecular communication. IEEE Commun. Surv. Tutor. **18**(3), 1887–1919 (2016)
5. Gohari, A., Mirmohseni, M., Nasiri-Kenari, M.: Information theory of molecular communication: directions and challenges. IEEE Trans. Mol. Biol. Multiscale Commun. **2**(2), 120–142 (2016)
6. Haselmayr, W., Aejaz, S.M.H., Asyhari, A.T., Springer, A., Guo, W.: Transposition errors in diffusion-based mobile molecular communication. IEEE Commun. Lett. **21**(9), 1973–1976 (2017)
7. Kilinc, D., Akan, O.B.: Receiver design for molecular communication. IEEE J. Sel. Areas Commun. **31**(12), 705–714 (2013)

8. Lin, L., Wu, Q., Liu, F., Yan, H.: Mutual information and maximum achievable rate for mobile molecular communication systems. IEEE Trans. Nanobiosci. **17**(4), 507–517 (2018)
9. Nakano, T., et al.: Random Cell Motion Enhances the Capacity of Cell-cell Communication (submitted)
10. Nakano, T., Okaie, Y., Kobayashi, S., Hara, T., Hiraoka, Y., Haraguchi, T.: Methods and applications of mobile molecular communication. Proc. IEEE **107**(7), 1442–1456 (2019)
11. Nakano, T.: Molecular communication: a 10 year retrospective. IEEE Trans. Mol. Biol. Multiscale Commun. **3**(2), 71–78 (2017)
12. Nakano, T., Eckford, A., Haraguchi, T.: Molecular Communication. Cambridge University Press, Cambridge (2013)
13. Okaie, Y., Nakano, T., Hara, T., Nishio, S.: Conclusion. Target detection and tracking by bionanosensor networks. SCS, pp. 59–65. Springer, Singapore (2016). https://doi.org/10.1007/978-981-10-2468-9_5